Computation of Free Energy

by **Wilfred F. van Gunsteren***[a]), **Xavier Daura**[b]), and **Alan E. Mark**[c])

[a]) Laboratory of Physical Chemistry, Swiss Federal Institute of Technology Zurich, ETH-Hönggerberg, CH-8093 Zurich (e-mail: wfvgn@igc.phys.chem.ethz.ch)
[b]) Institució Catalana de Recerca i Estudis Avançats (ICREA) and Institut of Biotechnologia i de Biomedicina, Universitat Autònoma de Barcelona, E-08193 Bellaterra
[c]) Department of Biophysical Chemistry, University of Groningen, NL-9747 AG Groningen

Dedicated to Professor *Dieter Seebach* on the occasion of his 65th birthday

Many quantities that are standardly used to characterize a chemical system are related to free-energy differences between particular states of the system. By statistical mechanics, free-energy differences may be expressed in terms of averages over ensembles of atomic configurations for the molecular system of interest. Here, we review the most useful formulae to calculate free-energy differences from ensembles generated by molecular simulation, illustrate a number of recent developments, and highlight practical aspects of such calculations with examples selected from the literature.

1. Introduction. – The probability of finding a molecular system in one state or the other is determined by the difference in free energy between those two states. As a consequence, free-energy differences may be directly related to a wide range of fundamental chemical quantities such as binding constants, solubilities, partition coefficients, and adsorption coefficients. By means of statistical mechanics, free-energy differences may also be expressed in terms of averages over ensembles of atomic configurations for the molecular system of interest. Such an ensemble can be generated by Monte Carlo (MC) or molecular-dynamics (MD) simulation techniques. However, despite its inherent simplicity, the computation of free-energy differences from molecular simulations in practice remains far from trivial. But, as techniques evolve over time and novel applications of existing approaches appear, our ability to use molecular-simulation techniques to predict important chemical phenomena continues to grow steadily.

The purpose of this paper is, therefore, twofold. First, we will introduce the most-useful formulae to calculate free-energy differences from ensembles generated by molecular simulation, and, second, we will illustrate a number of recent developments, as well as highlight practical aspects of such calculations, using examples selected from published works. For more-thorough reviews on the methodology to calculate free energy *via* molecular simulation, we refer to the literature [1–9]. In *Sect. 2*, the basic statistical mechanical description of the free energy of a system is given. In *Sect. 3*, a number of useful expressions for free-energy differences are reviewed. *Sect. 4* contains a discussion of a number of important technical issues, including choices to be made and pitfalls to be avoided in practical free-energy calculations. These are illustrated by examples primarily from our own work over many years. In *Sect. 5*, some conclusions are drawn.

2. A Statistical Mechanical Description of Free Energy. – In general terms, a microscopic description of a particular molecular system can be given in the form of a *Hamilton* operator or function. This is often simply expressed as the Hamiltonian $H(\mathbf{p},\mathbf{q})$ of the generalized coordinates $\mathbf{q}$ and their conjugate momenta $\mathbf{p}$. For example, the Hamiltonian for a classical system of N atoms, expressed in terms of the Cartesian coordinates $\mathbf{r} \equiv (\mathbf{r}_1, \mathbf{r}_2, ..., \mathbf{r}_N)$ and momenta $\mathbf{p} \equiv (\mathbf{p}_1, \mathbf{p}_2, ..., \mathbf{p}_N)$ of each of the atoms has the form

$$H(\mathbf{p},\mathbf{r}) = \sum_{i=1}^{N} \mathbf{p}_\mathbf{i}^2 / 2m_i + V(\mathbf{r}_1, \mathbf{r}_2, ..., \mathbf{r}_N), \tag{1}$$

where m_i is the mass of atom i, and $V(\mathbf{r})$ is the potential-energy function describing the interactions between the atoms.

In the canonical ensemble the fundamental formula for the *Helmholtz* free energy F is [10]

$$F(N, V, T) = -k_B T \ln\left[h^{-3N} \iint \exp\{-H(\mathbf{p},\mathbf{r})/k_B T\} d\mathbf{p} d\mathbf{r}\right], \tag{2}$$

where V is the volume of the system, T the absolute temperature, k_B *Boltzmann*'s constant, h *Planck*'s constant, and it is assumed that the N atoms are distinguishable. The essential difficulty in calculating the free energy of a system is already evident in *Eqn. 2*, which is dependent on a $6N$-dimensional integral to be carried out over phase space [11]. Since the integrand in *Eqn. 2* is always positive, and the logarithm is a monotonically increasing function, the calculated value of the free energy will become progressively lower, as more regions of phase space are included in the integration. This means that it is only possible to calculate the absolute free energy for a small number of model systems for which the total accessible phase space can be enumerated. In practice, only free-energy differences between two closely related states of a given system can be calculated by means of ensembles generated by molecular simulation.

Within the framework of statistical mechanics, a variety of formulae for determining the difference in free energy between two states of a system, or the projection of such a difference in free energy along a spatial (reaction) coordinate or a coordinate in parameter space, can be derived. The different formulations available are all equivalent within the limit of infinite sampling of phase space. In practice, however, as only a tiny part of the total phase space accessible to a realistic system can ever be sampled by molecular-simulation techniques, there are often significant differences in accuracy between the free-energy estimates obtained from different formulae.

3. Methods to Compute Free-Energy Differences. – Below, we list the most useful statistical mechanical formulae and computational methods to obtain the difference in free energy

$$\Delta F_{BA} \equiv F_B - F_A \equiv F(B) - F(A) \tag{3}$$

between two states A and B of a molecular system.

3.1. *Direct Counting.* The most straightforward way to determine the difference in free energy between two states of a system is simply to count the number of

configurations in the corresponding states. For example, in the case of binding constants, this involves simply counting the number of bound configurations N_B and the number of unbound configurations N_A in an ensemble generated during a MD or MC simulation, with the difference in free energy being given by

$$\Delta F_{BA} = -k_B T \ln[N_B/N_A]. \tag{4}$$

This technique is only appropriate, when both bound and unbound configurations occur with sufficient frequency in the ensemble to obtain reliable statistics, *i.e.*, when the ΔF_{BA} is small, and the barrier that determines the rate of binding and release is also small. An example of the use of *Eqn. 4* to determine the difference in free energy of binding for a pair of chirally related molecules can be found in [12]. Direct counting has the advantage that it does not depend on the definition of a reaction coordinate. It is particularly well-suited to situations in which the end states are themselves ensembles of structures, such as in the study of peptide folding [13]. By simply counting the proportion of configurations that satisfy a particular objective criterion such as the root-mean-square deviation (RMSD) from a particular folded conformation, it is possible to make a direct comparison between the apparent stability of the peptide in a simulation and experimental data.

3.2 *Integration Methods.* Integration methods determine the change in free energy between two states of a system from the integral of the work required to go from an initial state to a final state *via* a reversible path. The path itself may be physical or non-physical.

3.2.1. *Temperature Integration.* Dividing *Eqn. 2* by T and taking the partial derivative with respect to $1/T$ at constant N and V we find

$$\frac{\partial(F/T)}{\partial(1/T)} = \langle H \rangle, \tag{5}$$

where $\langle \cdots \rangle$ denotes a canonical ensemble average. The free-energy difference of a molecular system at two different temperatures T_A and T_B can then be found by means of the temperature-integration formula

$$F(T_B)/T_B - F(T_A)/T_A = \int_{1/T_A}^{1/T_B} \langle H \rangle d(1/T). \tag{6}$$

The ensemble averages $\langle H \rangle$ of the total energy can be determined from constant-volume simulations at a series of temperatures between T_A and T_B, and the integral in *Eqn. 6* evaluated numerically.

3.2.2. *Pressure Integration.* The partial derivative of the free energy F with respect to the volume V at constant N and T is equal to the negative of the pressure P [10],

$$\frac{\partial F}{\partial V} = -P. \tag{7}$$

The free-energy difference of a molecular system at two different volumes V_A and V_B can then be found by means of the pressure-integration formula

$$F(V_{\mathrm{B}}) - F(V_{\mathrm{A}}) = -\int_{V_{\mathrm{A}}}^{V_{\mathrm{B}}} P dV. \tag{8}$$

The pressure of the system can be determined from constant-temperature simulations at a series of volumes between V_{A} and V_{B}, and the integral in *Eqn. 8* evaluated numerically.

3.2.3. *Thermodynamic Integration.* A generalized form of the integration methods described above can be achieved by the introduction of an arbitrary coupling parameter linking two or more states of the system. With this approach, the Hamiltonian $H(\mathbf{p},\mathbf{r})$ is made a function of a coupling parameter λ to give $H(\mathbf{p},\mathbf{r};\lambda)$. The coupling parameter is chosen such that when $\lambda = \lambda_{\mathrm{A}}$ the Hamiltonian of the molecular system corresponds to that of state A, *i.e.*, $H(\mathbf{p},\mathbf{r};\lambda_{\mathrm{A}}) = H_{\mathrm{A}}(\mathbf{p},\mathbf{r})$, and when $\lambda = \lambda_{\mathrm{B}}$ the Hamiltonian of the system corresponds to that of state B, *i.e.*, $H(\mathbf{p},\mathbf{r};\lambda_{\mathrm{B}}) = H_{\mathrm{B}}(\mathbf{p},\mathbf{r})$. If the Hamiltonian is a function of λ the free energy *Eqn. 2* will also be a function of λ, and the derivative of the free energy with respect to λ will be given by

$$\frac{dF(\lambda)}{d\lambda} = \left\langle \frac{\partial H(\lambda)}{\partial \lambda} \right\rangle_{\lambda}. \tag{9}$$

From this, it follows directly that the free-energy difference between state A and state B of a molecular system is given by

$$F(\lambda_{\mathrm{B}}) - F(\lambda_{\mathrm{A}}) = \int_{\lambda_{\mathrm{A}}}^{\lambda_{\mathrm{B}}} \left\langle \frac{\partial H(\lambda)}{\partial \lambda} \right\rangle_{\lambda} d\lambda, \tag{10}$$

which is the so-called thermodynamic-integration formula [14]. The ensemble average $\langle \partial H/\partial \lambda \rangle$ is most commonly determined from simulations at a series of λ values between λ_{A} and λ_{B}, and the integral in *Eqn. 10* evaluated numerically. In many applications, the coupling-parameter approach is used to link two physical states *via* a nonphysical pathway with λ, for example, referring to a coordinate in parameter space. The choice of λ is, however, arbitrary, and λ may equally well refer to a spatial coordinate. In either case, the functional dependence of the system on λ effectively describes the pathway from the initial to the final state.

3.3. *Perturbation Approaches.* 3.3.1. *Multistep Perturbation.* An alternative to thermodynamic integration is to adopt a perturbation approach. For example, if in the coupling parameter approach the derivative of the free energy with respect to λ is expressed in terms of a finite difference

$$\frac{dF(\lambda)}{d\lambda} = [F(\lambda + \Delta\lambda) - F(\lambda)]/\Delta\lambda, \tag{11}$$

it may be readily shown, with *Eqn. 2* and after rearrangement of factors that

$$\frac{dF(\lambda)}{d\lambda} = -k_B T \ln \left[\langle \exp\{-(H(\lambda + \Delta\lambda) - H(\lambda))/k_B T\} \rangle_{\lambda} \right]/\Delta\lambda. \tag{12}$$

With a series of λ values, $\Delta\lambda$ apart, between λ_{A} and λ_{B}, we find

$$F(\lambda_{\mathrm{B}}) - F(\lambda_{\mathrm{A}}) = \sum_{\lambda=\lambda_{\mathrm{A}}}^{\lambda_{\mathrm{B}}-\Delta\lambda} -k_B T \ln \left[\langle \exp\{-(H(\lambda + \Delta\lambda) - H(\lambda))/k_B T\} \rangle_{\lambda} \right]. \tag{13}$$

The ensemble average in *Eqn. 13* can be determined from simulations at a series of λ values between λ_A and λ_B, and the sum of the logarithms taken to evaluate the free-energy difference.

3.3.2. *Single-Step Perturbation.* In principle, *Eqn. 13* holds for any value of $\Delta\lambda$ so long as the ensemble average indicated by the angular brackets converges. Thus, if the difference between the Hamiltonians at λ_A and λ_B is small, or more precisely, if there is sufficient overlap between the low-energy configurations of the ensembles belonging to λ_A and λ_B, one may obtain the free-energy difference F_{BA} from a one-step perturbation [15]:

$$F(\lambda_B) - F(\lambda_A) = -k_B T \ln[\langle \exp\{-(H(\lambda_B) - H(\lambda_A))/k_B T\}\rangle_{\lambda_A}]. \tag{14}$$

The particle-insertion method of *Widom* [16] is an application of *Eqn. 14* to obtain the excess chemical potential of a system in state A by inserting a test particle (state B).

3.4. *Extrapolation.* If the Hamiltonians at λ_A and λ_B are closely related, one may use a *Taylor*-series expansion for $F(\lambda)$ about λ_A

$$F(\lambda_B) - F(\lambda_A) = \sum_{n=1}^{\infty} \frac{d^n F(\lambda)}{d\lambda^n}\bigg|_{\lambda=\lambda_A} (\lambda_B - \lambda_A)^n/n!, \tag{15}$$

in which the successive derivatives of the free energy with respect to λ can be expressed as ensemble averages of the successive partial derivatives of the Hamiltonian with respect to λ [17]. The first derivative is given by *Eqn. 9*, the second by

$$\frac{d^2 F(\lambda)}{d\lambda^2} = \left\langle \frac{\partial^2 H(\lambda)}{\partial\lambda^2} \right\rangle_\lambda - (k_B T)^{-1} \left\langle \left[\frac{\partial H(\lambda)}{\partial\lambda} - \left\langle \frac{\partial H(\lambda)}{\partial\lambda} \right\rangle_\lambda \right]^2 \right\rangle_\lambda. \tag{16}$$

Higher derivatives up to fifth order can be found in [17]. Inserting the ensemble average expressions for the successive derivatives of $F(\lambda)$ at $\lambda = \lambda_A$ in *Eqn. 15*, one obtains the extrapolation formula for the free-energy difference ΔF_{BA}.

3.5. *Potential of Mean Force, Umbrella Sampling.* The difference in free energy between two states of a molecular system is a single number. Often, we would like to know how the free energy of a system changes as a function of a particular coordinate within the system, most commonly a spatial coordinate. In other words, we would like to project the free energy onto a hypersurface in configuration (or parameter) space:

$$R(\mathbf{r}) = R(\mathbf{r}_1, \mathbf{r}_2, \ldots, \mathbf{r}_N). \tag{17}$$

Such a hypersurface is commonly called a reaction coordinate and, in configurational space, is a function of the positions of the atoms in the system. The free energy as a function of the reaction coordinate R', or the potential of mean force, then becomes [7]

$$F(R') = -k_B T \ln P(R') + \text{constant}, \tag{18}$$

where $P(R')$ is the probability of finding the system lying on the reaction coordinate. In principle, there are three possibilities to compute the potential of mean force $F(R')$:

1) From a normal simulation, one can select those configurations that satisfy $R' = R(\mathbf{r})$ for any value R' of the R coordinate. The relative probability $P(R')$ follows then directly from the relative frequency with which the selected configurations occur, and the free-energy profile $F(R')$ can be obtained with *Eqn. 18*. This method yields reliable values for $F(R')$ only for those R-coordinate values that occur frequently during the simulation: R values that correspond to high-energy configurations, in particular, will be poorly sampled.

2) To improve the sampling of specific regions of the R coordinate, a restraining or umbrella potential [18], $V_r(R(\mathbf{r});R_0)$ can be added to the Hamiltonian $H(\mathbf{p},\mathbf{r})$. For example, the function

$$V_r(R(\mathbf{r}); R_0) = \frac{1}{2}K_r[R(\mathbf{r}) - R_0]^2 \tag{19}$$

will restrain the molecular configurations harmonically to the R-coordinate value R_0. This (strongly) enhances (if $K_r > 0$) the probability of finding configurations with $R(\mathbf{r}) \approx R_0$ in the restrained simulation. The unrestrained R-coordinate probability $P(R')$ can be expressed in terms of the restrained probability $P_r(R')$ and a restrained ensemble average $\langle \cdots \rangle_r$ [7]

$$P(R') = P_r(R')\langle\exp\{V_r(R; R_0)/k_B T\}\rangle_r^{-1} \exp\{V_r(R'; R_0)/k_B T\}. \tag{20}$$

Using *Eqn. 18*, we find

$$F(R') = -k_B T \ln P_r(R') - V_r(R'; R_0) + \text{constant}, \tag{21}$$

the potential of mean-force formula to be used in conjunction with umbrella sampling.

3) Alternatively, the system can be forced to move along the R coordinate by performing a simulation in which the system is constrained to the hypersurface $R(\mathbf{r}) = R_c$. The derivative of the free energy of the constrained system with respect to R then becomes [7]

$$\frac{dF_c(R)}{dR} = -\langle f_c(R)\rangle_c, \tag{22}$$

where the symbol $\langle \cdots \rangle_c$ denotes an ensemble average over the constrained simulation. The constraint force, *i.e.*, the force that is to be added to the non-constrained force in order to have the trajectory satisfy the constraint $R(\mathbf{r}) = R_c$, is denoted by $f_c(R)$. This force can be directly obtained from the constrained simulation. Using *Eqn. 22*, we find

$$F_c(R_B) - F_c(R_A) = -\int_{R_A}^{R_B} \langle f_c(R)\rangle_c dR, \tag{23}$$

the potential of mean force formula to be used in conjunction with constrained simulation to determine a free-energy profile.

3.6. *Free-Energy Components: Entropy and Enthalpy.* From classical thermodynamics, we know that the change in free energy can be expressed in terms of two components, a change in internal energy and a change in entropy, as follows:

$$\Delta F_{\mathrm{BA}} = \Delta E_{\mathrm{BA}} - T\Delta S_{\mathrm{BA}}, \tag{24}$$

No other physically meaningful separation of the free energy into components is possible either experimentally or theoretically [19][20]. The reason for calculating the overall change in free energy rather than the change in the internal energy and the entropy separately can be readily seen from the following formulae. The change in internal energy when going from a state A to a state B is given by

$$\Delta E_{\mathrm{BA}} = E(\lambda_{\mathrm{B}}) - E(\lambda_{\mathrm{A}}) = \langle H(\lambda_{\mathrm{B}})\rangle_{\lambda_{\mathrm{B}}} - \langle H(\lambda_{\mathrm{A}})\rangle_{\lambda_{\mathrm{A}}}. \tag{25}$$

The change in entropy according to the thermodynamic-integration formalism is given by

$$\Delta S_{\mathrm{BA}} = \left(k_B T^2\right)^{-1} \int_{\lambda_{\mathrm{A}}}^{\lambda_{\mathrm{B}}} \left[\langle H(\lambda)\rangle_\lambda \left\langle \frac{\partial H(\lambda)}{\partial \lambda} \right\rangle_\lambda - \left\langle H(\lambda)\frac{\partial H(\lambda)}{\partial \lambda} \right\rangle_\lambda \right] d\lambda. \tag{26}$$

Thus, while the change in free energy can be expressed solely in terms of the interactions that are perturbed in going from the A state to the B state as in *Eqn. 10*, the change in internal energy and the change in entropy are dependent on the total Hamiltionian. This makes the differences in internal energy and entropy fundamentally more difficult to determine than differences in free energy. Nevertheless, in certain cases it is highly desirable to determine the entropy of a system. For example, to understand whether a particular process is entropically or enthalpically driven. In such cases one can place an upper bound on the entropy by using the formalism introduced by *Schlitter* [21], who showed that
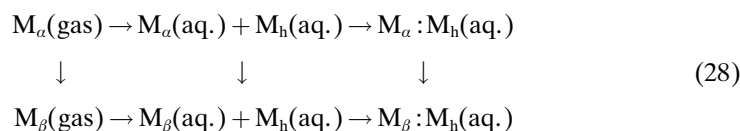
$$S < \frac{1}{2} k_B \ln \det \left[\mathbf{1} + \frac{k_B T e^2}{h^2} \mathbf{M}\boldsymbol{\sigma} \right], \tag{27}$$

where e is *Euler*'s number, $\hbar$ is Planck's constant divided by 2π, $\mathbf{M}\boldsymbol{\sigma}$ represents the mass-weighted covariance matrix of the atom-positional fluctuations, and the other symbols are as defined previously. *Eqn. 27* is based on the approximation that each degree of freedom can be represented by a quantum-mechanical harmonic oscillator. Although approximate, *Eqn. 27* has been shown to give reasonably accurate estimates for the entropy for a number cases that can be determined analytically [22]. An example of the use of *Eqn. 27* to understand the nature of entropic contributions to peptide stability is given in [23].

4. Computation of Free-Energy Differences in Practice. – In this section, we briefly discuss a number of technical issues that are important to achieve reliable results in practical free-energy calculations. The points are illustrated with examples from our own published work, which could be consulted for further details.

4.1. *Choice of End States, Pathways and Cycle.* Beside the most-appropriate statistical mechanical formula, the computation of a free-energy difference generally involves three basic choices: *i*) the definition of the end states A and B, *ii*) the pathway that will connect them, and *iii*) the definition of one or more thermodynamic cycles of which they are a part. Since the free energy is a thermodynamic state

function, a change in free energy ΔF_{BA} will be independent of the path connecting states A and B as long as the system is in equilibrium, and the change is performed in a reversible way, and, along a closed path or cycle, $\Delta F_{cycle} = 0$. As the efficiency of a particular calculation depends greatly on the pathway that is chosen and the nature of the changes imposed on the system, the use of thermodynamic cycles allows the selection of more efficient (often nonphysical) paths. For example, complexation (indicated by the symbol :) of two different guest molecules M_α and M_β to a host molecule M_h in aqueous solution, or the hydration of these guest molecules, can be described by the cycles

$$
\begin{array}{ccc}
M_\alpha(\text{gas}) \rightarrow M_\alpha(\text{aq.}) + M_h(\text{aq.}) \rightarrow M_\alpha : M_h(\text{aq.}) \\
\downarrow \qquad\qquad \downarrow \qquad\qquad \downarrow \\
M_\beta(\text{gas}) \rightarrow M_\beta(\text{aq.}) + M_h(\text{aq.}) \rightarrow M_\beta : M_h(\text{aq.})
\end{array}
\qquad (28)
$$

The relative free energies of hydration of M_α and M_β can be obtained by performing free-energy simulations either along the horizontal arrows or along the vertical ones. The possibility to compute ΔF for all legs of a cycle, however, also offers the opportunity to obtain a lower bound on the error: ΔF_{cycle}.

As stated above, the accuracy of a free-energy computation can be enhanced by a judicious choice of end states, pathways, and cycles. This is because the proper sampling of the ensembles and the convergence of the ensemble averages in *Eqns. 10*, *13 – 16*, *18*, *20*, *21*, *23*, and *25 – 27* are very much dependent on: *1*) the expression to be averaged, *2*) the particular point along the pathway (λ value or R-coordinate value), *3*) the pathway chosen to connect states A and B in a cycle, *4*) the λ or R dependence of the Hamiltonian.

For example, *Fig. 1* illustrates the convergence of the first (*Eqn. 9*), second (*Eqn. 16*) and higher-order derivatives of the free energy *F*. The figure actually shows the *Gibbs* free energy *G* as a function of time obtained by extrapolating from an ensemble at $\lambda = \lambda_A$ with *Eqn. 15* for a change involving the inversion of a solute dipole in a periodic box with 510 H_2O molecules [17]. As higher-order derivatives of the free energy are included in the extrapolation, the *Gibbs* free energy converges more slowly. By way of contrast, *Fig. 2* shows the convergence properties of *Eqn. 14* for exactly the same system. The value $\lambda = 1$ (*i.e.* $\lambda = \lambda_B$) represents the dipole inversion [24]. Every time a configuration is sampled in the ensemble generated with $H(\lambda_A = 0)$ that has a low energy $H(\lambda_B)$ for state B, the free-energy difference *Eqn. 14* drops sharply. Clearly, the convergence properties of linear combinations of derivatives of *H*, *Eqn. 15*, differ greatly from the convergence properties of the exponential of a difference in Hamiltonians, *Eqn. 14*, even though, in the limit of infinite sampling, the two approaches are equivalent.

Fig. 3 illustrates the dependence of the convergence of the ensemble average (*Eqn. 9*) upon the λ value or R-coordinate value. In this case, λ is proportional to the radius of a cavity in a periodic box with 512 H_2O molecules for which the hydration (excess) free energy was calculated [25]. The relative accuracy of the derivative of the excess *Gibbs* free energy falls to less than 2.5% within 100 ps for the two smallest and two largest radii (*Fig. 3a*, *b*, *e*, and *f*). This accuracy is achieved only after 250 ps for the
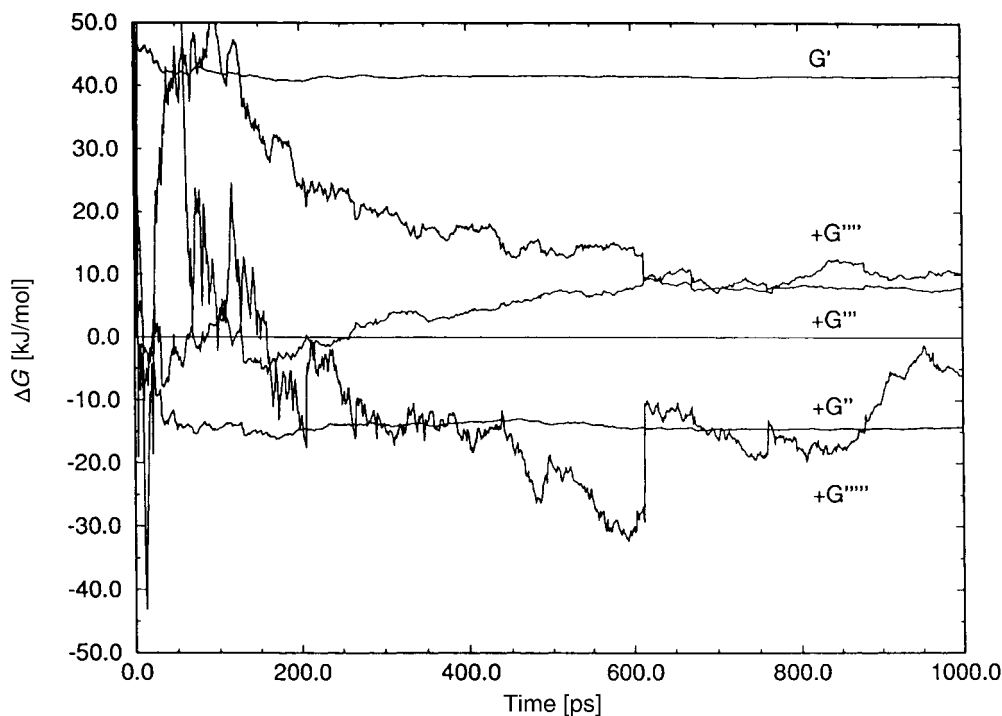
Fig. 1. *Running average of the extrapolated* Gibbs *free-energy change ΔG for the inversion of a dipole in H₂O as calculated with the free-energy extrapolation* Eqn. 15. The different curves represent successive additions of higher derivatives in *Eqn. 15*. The line at $\Delta G = 0$ is the exact result. Results taken from [17].

two intermediate radii, which indicates instabilities in the H_2O shell for these particular cavity sizes.

Fig. 4 illustrates how the choice of the pathway to connect states X and Y affects the accuracy of ΔF_{YX} [26]. In this example, the free energy was calculated by means of a 'slow growth' procedure in which the system was changed continuously throughout the simulation. Path *A* used a linear combination of the two end states to achieve the transition from state X, a model of butane preferring the *trans*-conformation, to state Y, an artificial butane preferring a *gauche* conformation. By Path *A*, a value of $\Delta F_{YX} = 1.66 \pm 3.2$ kJ mol^{-1} was obtained by averaging the result with 50 ps of simulation in the forward direction, and the result with 50 ps of simulation in the reverse direction. The error is half the difference between the forward and reverse directions. With the same path but 500 ps of simulation in each direction $\Delta F_{YX} = 1.72 \pm 1.2$ kJ mol^{-1} (not shown in *Fig. 4*). Paths *B* and *C* represent alternative indirect pathways along which first (stage *I*) the potential-energy barriers are reversibly reduced by a factor ½ or ¼, respectively, then the change of Hamiltonian from X to Y is made (stage *II*), and finally the reduction of the potential-energy barriers is reversed (stage *III*). Path *B* yields a $\Delta F_{YX} = 1.33 \pm 0.8$ kJ mol^{-1} with a total of 60 ps of simulation in each direction or $\Delta F_{YX} = 1.60 \pm 0.15$ kJ mol^{-1} with 200 ps of simulation in each direction (not shown in
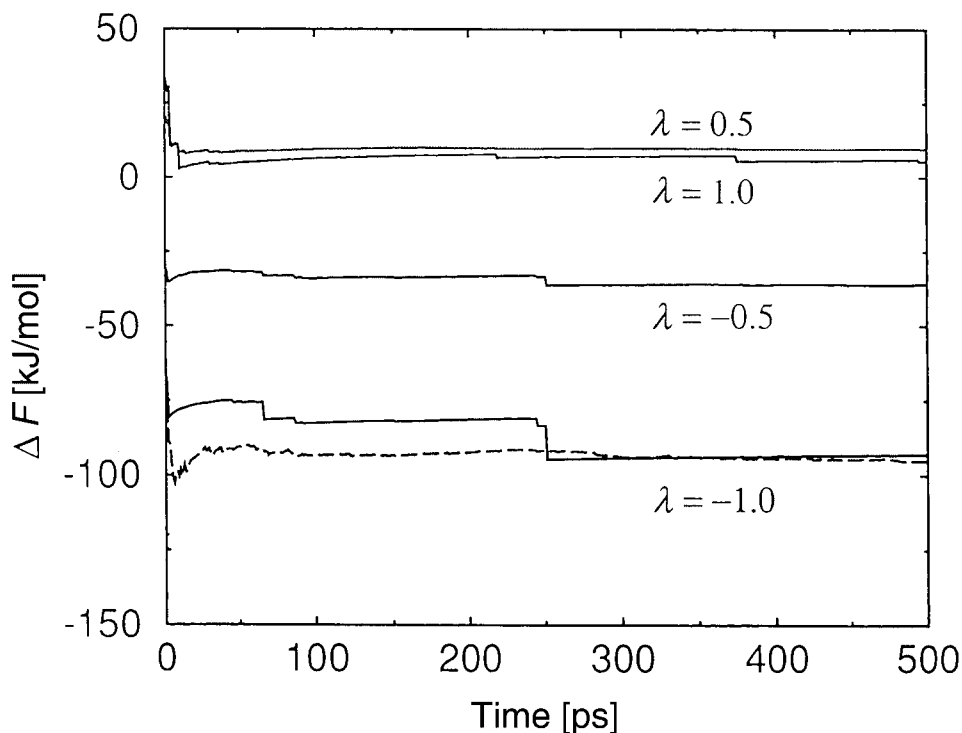
Fig. 2. *Running average of the extrapolated free-energy change* ΔF *for the inversion* ($\lambda = 1$) *or the doubling* ($\lambda = -1$) *of a dipole in* H_2O *as calculated with the one-step perturbation* Eqn. 14. For $\lambda = -1$, the extrapolation result based on a *Taylor* series, *Eqn. 15*, truncated beyond the second-order term is also shown (dashed line). Results taken from [24].

Fig. 4). If a path is chosen for which the relaxation time of the system is minimal, the system will stay close to equilibrium and the error in ΔF_{YX} will be minimized.

The choice of the λ or R dependence of the Hamiltonian requires special care in cases where atoms or interaction sites are created or annihilated. The standard *Van der Waals* and electrostatic-interaction terms contain a singularity when the interparticle distance $r_{ij} = 0$. This may cause the ensemble averages in (10, 12 – 16) to diverge and the numerical integration of the equations of motion to become unstable during, *e.g.*, the initial phase of an atom being created [27]. Ignoring this singularity will potentially lead to erratic and unreliable estimates of free-energy differences. Many approaches have been proposed to avoid such problems, including nonlinear scaling of the potential and various schemes to 'protect' sites where atoms are to be created or annihilated [28]. The most effective approach is, however, to employ so-called soft-core nonbonded interaction terms, *e.g.*, for atom annihilation [27],
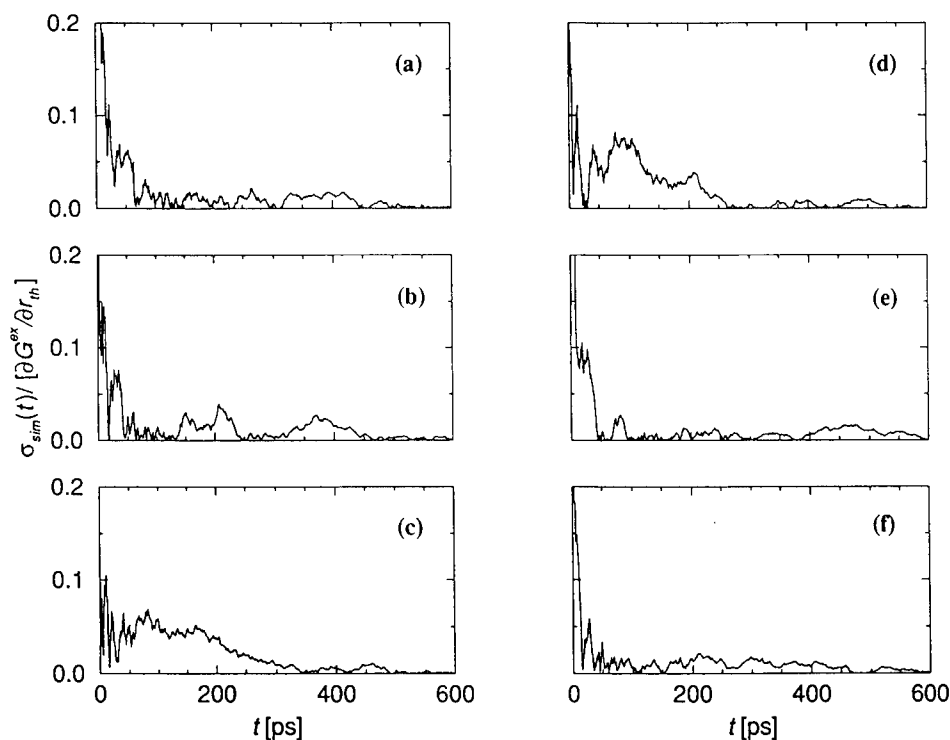
Fig. 3. *Estimate of the relative accuracy of the ensemble average of the excess hydration* Gibbs *free-energy derivative, as a function of simulation length for six cavities of different sizes in* H_2O. Cavity radii are: *a*) 0.25 nm, *b*) 0.30 nm, *c*) 0.325 nm, *d*) 0.35 nm, *e*) 0.375 nm, *f*) 0.40 nm. Results taken from [25].

$$V_{ij}(r_{ij};\lambda) = \lambda\left\{\frac{q_i q_j}{4\pi\varepsilon_0\varepsilon_r\left[\alpha_c(1-\lambda)^2+r_{ij}^2\right]^{1/2}}\right.$$

$$\left. + 4\varepsilon_{ij}\left[\frac{1}{\left[\alpha_{LJ}(1-\lambda)^2+\left(r_{ij}/\sigma_{ij}\right)^6\right]^2} - \frac{1}{\alpha_{LJ}(1-\lambda)^2+\left(r_{ij}/\sigma_{ij}\right)^6}\right]\right\}, \tag{29}$$

where $\varepsilon_o\,\varepsilon_r$ is the dielectric permittivity, q_i is the charge on atom i, and ε_{ij} and σ_{ij} are the *Lennard-Jones* interaction parameters for atom pair (i,j). The constants α_c and α_{LJ} govern the softness of the interaction [29]. For $\lambda=1$ or $\alpha_c=\alpha_{LJ}=0$, the original interaction is obtained, and for $\alpha_c > 0$ and $\alpha_{LJ} > 0$, the interaction becomes softer for decreasing λ, as shown in *Fig. 5*. For atom creation comparable forms can be formulated [30].

Finally, if the Hamiltonian depends parametrically on constraints, and these constraints are made λ- or R-dependent, the contribution of the constraint forces to the free-energy change must be evaluated [3][7][30].
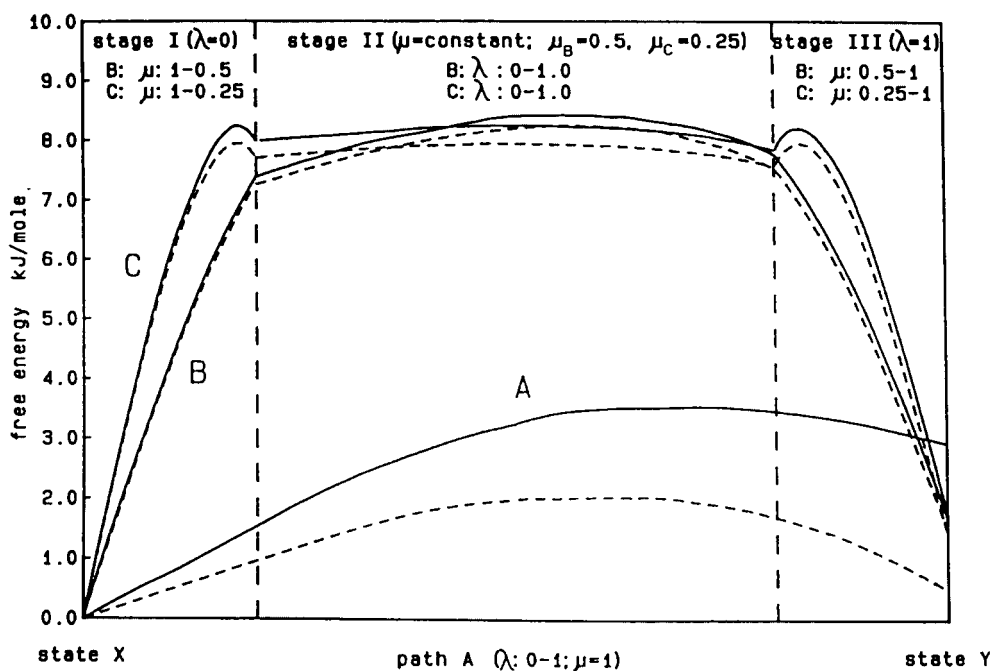
Fig. 4. *A comparison of the calculated free-energy changes associated with the change of a model butane molecule* (state X) *into an artificial butane molecule preferring* gauche *states* (state Y) *in liquid butane, as calculated with thermodynamic integration for different pathways* A, B *and* C. Pathway *A* is direct, whereas pathways *B* and *C* involve a reduction of the potential-energy barriers in stage I and a rebuilding of them in stage III. The difference between solid lines (forward mutation) and dashed lines (backward mutation) is indicative of the sampling error. Results taken from [26].

4.2. *Integration over λ or* R *Coordinate.* A free-energy-difference calculation often involves a numerical integration over a range of parameter values (see *Eqns. 6, 8, 10,* and *23*). Various numerical-integration formulae, such as *Gauss-Legendre* quadrature, *Simpson*'s rule, or trapezoidal approximation can be used [31][32]. These methods often assume, however, that any uncertainty is evenly distributed along the integrand. In free-energy calculations, this is often not the case. The important point is to include more function values in the parts of the λ or R domain where the function to be integrated is rapidly varying. This is illustrated in *Fig. 6* for a thermodynamic-integration calculation of the free-energy difference between N-acetyltryptamine and *N*-methyl-3-(indol-3-yl)propanamide in H_2O and in $CHCl_3$ [32]: the regions around $\lambda = 0.1$ and $\lambda = 0.9$ need more-closely-spaced λ values.

4.3. *One-Step Perturbation and Extrapolation.* The difference in free energy between a particular reference state A and any other state B of a system can be determined with *Eqn. 14*, when the equilibrium ensemble corresponding to $H(\lambda_A)$ is *completely* known. Thus, a single simulation of the reference state A can, in principle, be used to estimate free-energy differences to a manifold of different states B. However, to obtain a reliable estimate of the free-energy difference ΔF_{BA} with *Eqn. 14*,
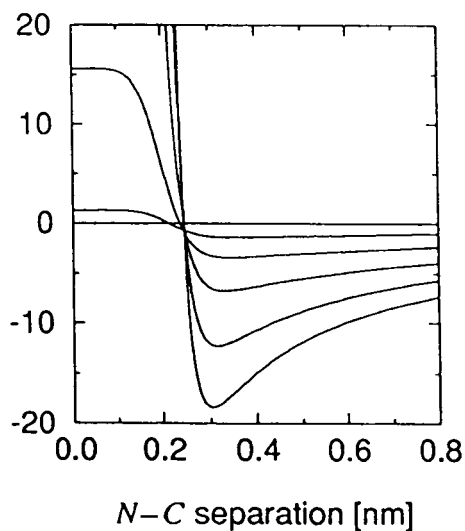
$$N-C \text{ separation [nm]}$$

Fig. 5. *Scaling of nonbonded interaction with the soft-core* Eqn. 29. The curves are the potential energy $V_{ij}(r_{ij}:\lambda)$ for $\lambda = 1.0, 0.8, 0.6, \ldots, 0.0$ (curves lying progressively closer to the *x*-axis at larger separations) as a function of the $N-C$ separation r_{ij}. The soft-core parameter values are $\alpha_c = 1 \text{ nm}^2$ and $\alpha_{LJ} = 0.3$. Results taken from [27].
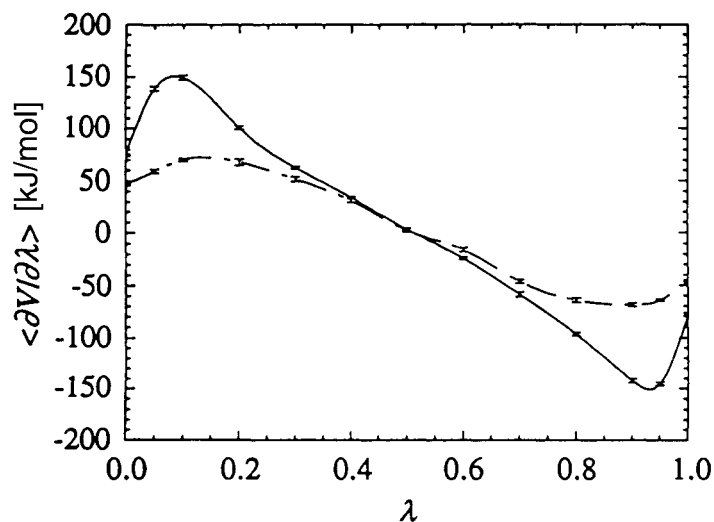
Fig. 6. *Ensemble averages of the derivative of the Hamiltonian with respect to λ for 13 λ values for the change of* N-*acetyltryptamine* $(\lambda = 0)$ *to* N-*methyl-3-(indol-3-yl)propanamide* $(\lambda = 1)$, *and cubic spline interpolations for the simulations in H_2O* (solid line) *and in $CHCl_3$* (dashed line). Results taken from [32].

low-energy configurations of the state defined by $H(\lambda_B)$ must be members of the ensemble of configurations generated with $H(\lambda_A)$. Such overlap of the reference and target ensembles does not occur, when atoms are either created or deleted, or for mutations involving significant reorganization of the environment. As a consequence, the change from λ_A to λ_B is normally split into a number of steps, as indicated in *Eqn. 13*.

However, by means of an appropriately modified Hamiltonian $H(\lambda_A)$ that is biased to increase sampling in a localized region, for example, by placing soft-core interaction sites of type (*Eqn. 29*) at locations where atoms are to be created or annihilated, it is possible to predict the differences in binding or hydration free energies for a wide range of compounds from a single simulation of modest length. For example, hydration free-energy differences of a set of *para*-substituted phenols could be accurately estimated with a single 300-ps simulation [24]. Furthermore, hydration free energies for a range of different sized nonpolar compounds were also accurately estimated from a single 1 ns simulation of an appropriate reference state [33]. For highly polar molecules that can form specific H-bonding arrangements as well as inducing long-range order in the environment, longer simulations are required to sample a sufficient number of appropriate configurations for the results to be statistically reliable [33]. Orientational and translational sampling of the solute within the same solvent configuration can also be used to improve the statistics [34]. For example, *Table 1* shows hydration free energies for a series of polar and nonpolar compounds extrapolated from a single 1-ns simulation of a neutral cavity in H_2O. Despite the differences in size and polarity of the compounds, the average error (unsigned) between the exact (TI) results and the extrapolated values is only 2.0 kJ mol^{-1}. One-step perturbation or extrapolation methods can easily yield a 1000-fold increase in efficiency compared to multi-step perturbation or thermodynamic-integration calculations for sets of related compounds. As such, they are well-suited for the rapid *in-silico* screening of potential drug molecules [35], force-field refinement [36], or even for predicting the protonation state of peptides as a function of conformation [37].

4.4. *Cycle Closure.* When carrying out more than one change of a molecular system, *e.g.* from system A to B, and from A to C, the quality of the equilibration, sampling, and integration over λ can be tested by performing the change from system B to C, which closes a thermodynamic cycle

$$\Delta F_{BA} + \Delta F_{CB} + \Delta F_{AC} = 0. \tag{30}$$

Table 1. *Hydration Free Energies for a Series of Polar and Nonpolar Compounds Calculated with a One-Step Perturbation Approach*[a])

Solute	ΔF [kJ mol^{-1}]	
	Extrapolation	Exact (TI)
SPC/E H_2O	− 24.8	− 28.9
SPC H_2O	− 23.0	− 24.3
MeOH	− 19.0	− 20.8
EtOH	− 9.1	− 14.2
CHCl$_3$	3.5	− 0.7
CH$_4$	7.7	8.0
Me$_2$CH$_2$	10.8	9.0

[a]) The reference state was a neutral soft-core cavity. The extrapolated ΔF values were calculated with *Eqn. 14* based on a single 1-ns simulation of the reference state in a periodic box containing *ca.* 1000 SPC H_2O molecules. The ΔF for the creation of the reference cavity in H_2O was 10.9 kJ mol^{-1}. The exact results are obtained from multiple simulations (*ca.* 50-ps simulations at 10 to 21 λ values for each mutation) with thermodynamic integration (TI), *Eqn. 10*. Results taken from [34].

Table 2. *Total Changes in* Gibbs *Free Energy for Each of the Possible Three-Membered* (closed) *Cycles Involving Mutations between* p-*Chlorophenol,* p-*Methylphenol,* p-*Hydroxybenzonitrile and* p-*Methoxyphenol*[a])

Cycle	ΔG in H_2O		ΔG in α-CD		$\Delta\Delta G$ in α-CD/H_2O	
	9 points	12 points	9 points	12 points	9 points	12 points
$Cl \rightarrow Me \rightarrow CN \rightarrow Cl$	0.5	0.3	0.7	0.1	0.2	0.1
$Cl \rightarrow CN \rightarrow OMe \rightarrow Cl$	0.7	1.0	− 0.7	1.2	− 1.4	0.2
$Cl \rightarrow Me_{CN} \rightarrow OMe \rightarrow Cl$	1.9	0.2	3.2	1.7	1.3	1.5
$Me \rightarrow OMe \rightarrow CN \rightarrow Me$	0.7	− 1.1	3.2	0.4	2.5	1.5

[a]) From thermodynamic integration *Eqn. 10*. Simulations represent 9 or 12 λ points per leg of the cycle and for different environments (H_2O and α-cyclodextrin (α-CD) in H_2O). Values in kJ mol^{-1}. Results taken from [31].

Table 2 shows the values for the left side in *Eqn. 30* for each of the possible three-membered closed cycles involving mutations between *p*-chlorophenol, *p*-methylphenol, *p*-hydroxybenzonitrile, and *p*-methoxyphenol in H_2O and, when this guest molecule is bound to α-cyclodextrin (α-CD) in H_2O [31]. The numerical integration over λ was performed with 9 or 12 λ values (20-ps sampling in H_2O and 40-ps sampling when bound to α-CD) and a trapezoidal formula. Ideally, all values in *Table 2* should be zero. The ΔG values are a lower bound on the error of the different free-energy calculations. This is independent of the force field used. The $\Delta\Delta G$ values cannot be used for other than a lower-limit error estimate, since they are often reduced by compensation of errors.

4.5. *Potential of Mean-Force Calculation or Umbrella Sampling in Practice.* Umbrella sampling or constrained simulation along a chosen reaction coordinate or pathway is a useful technique to determine the free-energy difference between two states of a molecular system separated by an energy barrier [38]. However, only the free energy as function of the chosen R coordinate is obtained. The use of another R coordinate to connect the end states may lead to a different free-energy difference. Performing potential of mean-force calculations along different R coordinates leading to approximately equal end states may indicate the dependence of the free-energy differences obtained upon the chosen reaction coordinate [39].

When umbrella-sampling techniques are used, the choice of restraining term V_r ($R(\mathbf{r});R_0$) in the Hamiltonian will greatly affect the sampling efficiency [40]. If the R coordinate is a linear combination of generalized coordinates, the proper choice of the restraining term requires care [41]. Finally, a potential of mean force along two reaction coordinates can be obtained by an extension of the one-dimensional *Eqn. 18* to two dimensions [42]. Determining a potential of mean force in more than two dimensions becomes an almost impossible task due to the scaling of the computational effort as n^d, where n is the number of points per R coordinate to be sampled with individual simulations, and d is the number of independent R coordinates.

5. Conclusions. – The most useful formulae and techniques to compute free-energy differences by molecular simulation have been reviewed, and a number of practical aspects of such calculations have been illustrated with examples from the literature. To obtain reliable estimates of the difference in free energy between two states of a system three crucial conditions must be met: *i*) the simulation must be performed with a sufficiently

accurate force field; *ii*) the system must be in proper equilibrium at all times; *iii*) a set of configurations representative of the complete equilibrium ensemble must be sampled at each point. In addition, the selection of the most appropriate statistical mechanical formula for a particular application, together with the incorporation of a judiciously chosen biasing function into the Hamiltonian to speed equilibration and promote sampling, may greatly enhance the accuracy and efficiency of free-energy calculations.

REFERENCES

[1] M. Mezei, D. L. Beveridge, *Ann. N. Y. Acad. Sci.* **1986**, *482*, 1.
[2] D. L. Beveridge, F. M. DiCapua, *Annu. Rev. Biophys. Biophys. Chem.* **1989**, *18*, 431.
[3] W. F. van Gunsteren, in 'Computer Simulation of Biomolecular Systems, Theoretical and Experimental Applications', Eds. W. F. van Gunsteren, P. K. Weiner, ESCOM Science Publishers, Leiden, 1989, Vol. 1, pp. 27–59.
[4] D. Frenkel, in 'Computer Simulation in Material Science', NATO ASI Series E205, Eds. M. Meyer, V. Pontikis, Kluwer Academic Publishers, Dordrecht, 1991, pp. 85–117.
[5] T. P. Straatsma, J. A. McCammon, *Annu. Rev. Phys. Chem.* **1992**, *43*, 407.
[6] P. M. King, in 'Computer Simulation of Biomolecular Systems, Theoretical and Experimental Applications', Eds. W. F. van Gunsteren, P. K. Weiner, A. J. Wilkinson, ESCOM Science Publishers, Leiden, 1993, Vol. 2, pp. 267–314.
[7] W. F. van Gunsteren, T. C. Beutler, F. Fraternali, P. M. King, A. E. Mark, P. E. Smith, in 'Computer Simulation of Biomolecular Systems, Theoretical and Experimental Applications', Eds. W. F. van Gunsteren, P. K. Weiner, A. J. Wilkinson, ESCOM Science Publishers: Leiden, 1993, Vol. 2, pp. 315–348.
[8] T. P. Straatsma, in 'Reviews in Computational Chemistry', Eds. K. B. Lipkowitz, D. B. Boyd, VCH Publishers, New York, 1996, Vol. 9, pp. 81–127.
[9] A. E. Mark, in 'Encyclopedia of Computational Chemistry', Eds. P. von Ragué Schleyer, N. L. Allinger, T. Clark, J. Gasteiger, P. A. Kollman, H. F. Schaefer III, P. R. Schreiner, John Wiley & Sons, Chichester, 1998, Vol. 2, pp. 1070–1083.
[10] D. A. McQuarrie, 'Statistical Mechanics', Harper and Row, New York, 1976.
[11] H. J. C. Berendsen, in 'Proteins: Structure, Dynamics and Design', Eds. V. Enugopalakrishnan, P. R. Carey, I. C. P. Smith, S. G. Huang, A. C. Storer, ESCOM Science Publishers, Leiden, 1991, pp. 384–392.
[12] P. H. Hünenberger, J. K. Granwehr, J.-N. Aebischer, N. Ghoneim, E. Haselbach, W. F. van Gunsteren, *J. Am. Chem. Soc.* **1997**, *119*, 7533.
[13] X. Daura, W. F. van Gunsteren, A. E. Mark, *Proteins: Struct. Funct. Genet.* **1999**, *34*, 269.
[14] J. G. Kirkwood, *J. Chem. Phys.* **1935**, *3*, 300.
[15] R. Zwanzig, *J. Chem. Phys.* **1954**, *22*, 1420.
[16] B. Widom, *J. Chem. Phys.* **1963**, *39*, 2808.
[17] P. E. Smith, W. F. van Gunsteren, *J. Chem. Phys.* **1994**, *100*, 577.
[18] G. M. Torrie, J. P. Valleau, *J. Comput. Phys.* **1977**, *23*, 187.
[19] A. E. Mark, W. F. van Gunsteren, *J. Mol. Biol.* **1994**, *240*, 167.
[20] P. E. Smith, W. F. van Gunsteren, *J. Phys. Chem.* **1994**, *98*, 13735.
[21] J. Schlitter, *Chem. Phys. Lett.* **1993**, *215*, 617.
[22] H. Schäfer, A. E. Mark, W. F. van Gunsteren, *J. Chem. Phys.* **2000**, *113*, 7809.
[23] H. Schäfer, X. Daura, A. E. Mark, W. F. van Gunsteren, *Proteins: Struct. Funct. Genet.* **2001**, *43*, 45.
[24] H. Liu, A. E. Mark, W. F. van Gunsteren, *J. Phys. Chem.* **1996**, *100*, 9485.
[25] T. C. Beutler, D. R. Béguelin, W. F. van Gunsteren, *J. Chem. Phys.* **1995**, *102*, 3787.
[26] A. E. Mark, W. F. van Gunsteren, H. J. C. Berendsen, *J. Chem. Phys.* **1991**, *94*, 3808.
[27] T. C. Beutler, A. E. Mark, R. C. van Schaik, P. R. Gerber, W. F. van Gunsteren, *Chem. Phys. Letters* **1994**, *222*, 529.
[28] J. W. Pitera, W. F. van Gunsteren, *Mol. Simul.* **2002**, *28*, 45.
[29] A. E. Mark, Y. Xu, H. Liu, W. F. van Gunsteren, *Acta Biochim. Polonica* **1995**, *42*, 525.
[30] W. F. van Gunsteren, S. R. Billeter, A. A. Eising, P. H. Hünenberger, P. Krüger, A. E. Mark, W. R. P. Scott, I. G. Tironi, 'Biomolecular Simulation: The GROMOS96 Manual and User Guide', Vdf Hochschulverlag AG an der ETHZ, Zürich, 1996.

[31] A. E. Mark, S. P. van Helden, P. E. Smith, L. H. M. Janssen, W. F. van Gunsteren, *J. Am. Chem. Soc.* **1994**, *116*, 6293.

[32] X. Daura, P. H. Hünenberger, A. E. Mark, E. Querol, F. X. Avilés, W. F. van Gunsteren, *J. Am. Chem. Soc.* **1996**, *118*, 6285.

[33] H. Schäfer, W. F. van Gunsteren, A. E. Mark, *J. Comput. Chem.* **1999**, *20*, 1604.

[34] J. W. Pitera, W. F. van Gunsteren, *J. Phys. Chem. B* **2001**, *105*, 11264.

[35] B. C. Oostenbrink, J. W. Pitera, M. M. H. van Lipzig, J. H. N. Meerman, W. F. van Gunsteren, *J. Med. Chem.* **2000**, *43*, 4594.

[36] A. Villa, A. E. Mark, *J. Comput. Chem.*, submitted.

[37] R. Bürgi, F. Läng, W. F. van Gunsteren, *Mol. Simul.* **2001**, *27*, 215.

[38] R. Zangi, H. Kovacs, W. F. van Gunsteren, J. Johansson, A. E. Mark, *Proteins: Struct. Funct. Genet.* **2001**, *43*, 395.

[39] F. Fraternali, W. F. van Gunsteren, *Biopolymers* **1994**, *34*, 347.

[40] T. C. Beutler, W. F. van Gunsteren, *J. Chem. Phys.* **1994**, *100*, 1492.

[41] T. C. Beutler, W. F. van Gunsteren, *Chem. Phys. Lett.* **1995**, *237*, 308.

[42] T. C. Beutler, T. Bremi, R. R. Ernst, W. F. van Gunsteren, *J. Phys. Chem.* **1996**, *100*, 2637.